

A UNIVERSAL VELOCITY DISPERSION PROFILE FOR PRESSURE SUPPORTED SYSTEMS: EVIDENCE FOR MONDIAN GRAVITY ACROSS 7 ORDERS OF MAGNITUDE IN MASS

R. DURAZO¹, X. HERNANDEZ¹, B. CERVANTES SODI² AND S. F. SÁNCHEZ¹

¹Instituto de Astronomía, Universidad Nacional Autónoma de México, Apartado Postal 70–264 C.P. 04510 México D.F. México.

²Instituto de Radioastronomía y Astrofísica, Universidad Nacional Autónoma de México, Campus Morelia, 58090 Morelia, Michoacán, México.

Abstract

For any MONDian extended theory of gravity where the rotation curves of spiral galaxies are explained through a change in physics rather than the hypothesis of dark matter, a generic dynamical behavior is expected for pressure supported systems: an outer flattening of the velocity dispersion profile occurring at a characteristic radius, where both the amplitude of this flat velocity dispersion and the radius at which it appears are predicted to show distinct scalings with the total mass of the system. By carefully analyzing the dynamics of globular clusters and elliptical galaxies, we are able to significantly extend the astronomical diversity of objects in which MONDian gravity has been tested, from spiral galaxies, to the much larger mass range covered by pressure supported systems. We show that a universal projected velocity dispersion profile accurately describes various classes of pressure supported systems, and further, that the expectations of extended gravity are met, across seven orders of magnitude in mass. These observed scalings are not expected under dark matter cosmology, and would require particular explanations tuned at the scales of each distinct astrophysical system.

Keywords: gravitation — stars:kinematics and dynamics — galaxies:star clusters:general — galaxies: fundamental parameters — galaxies: kinematics and dynamics — galaxies: clusters: general

1. INTRODUCTION

Within the context of modified gravity theories constructed to yield galactic dynamics in the absence of dark matter, one of the most convincing supporting arguments comes from the success of MOND in reproducing rotation curves of spiral galaxies (Milgrom 1983; Swaters et al. 2010; McGaugh 2012). Both the flatness of the observed spiral rotation curves and the scaling of the asymptotic rotation with the fourth root of the total baryonic content, i. e. the Tully-Fisher relation, can be accurately reproduced across spiral galaxy sizes and types, as well as the overall shapes and correlations between observed features in the baryonic distribution and small kinematic irregularities (Sanders & McGaugh 2002; Famaey & McGaugh 2012; Rodrigues 2014; Lelli et al. 2016). However, such successful tests are restricted to the range of mass scales and morphology of spiral galaxies.

To test the validity (or lack thereof) of MONDian gravity schemes, it is desirable to extend the diversity of astrophysical systems over which these ideas can be probed. To do this, we give the expected kinematic profiles for two different types of pressure supported sys-

tems, astrophysical objects with baryonic masses spanning from $10^4 M_\odot$ for globular clusters, to $10^{11} M_\odot$ for elliptical galaxies.

By the term MONDian gravity we shall refer to any extended gravity theory where at $a > a_0$ scales Newtonian gravity is recovered, while the $a < a_0$ regime reproduces MOND dynamics, at the $v \ll c$ limit, where a_0 is Milgrom's acceleration of $1.2 \times 10^{-10} m/s^2$ (Bekenstein 2004; Capozziello & De Laurentis 2011; Mendoza et al. 2013; Verlinde 2016). Generically for such theories, beyond a radius given by $R_M = (GM/a_0)^{1/2}$, centrifugal equilibrium velocities will become flat at a level of $V = (GMa_0)^{1/4}$. Similarly, for pressure supported systems, beyond around R_M , velocity dispersion profiles will stop falling along Newtonian expectations and flatten out at a level of $\sigma_\infty = V/3^{1/2}$, with M the total baryonic mass of a rapidly converging astrophysical system (Milgrom 1984; Hernandez & Jimenez 2012).

Recently, McGaugh et al. (2016) and Lelli et al. (2016) used the SPARC rotation curve and photometry database, to show that the baryonic mass distribution alone directly determines the resulting acceleration, along Newtonian expectations in the high acceleration

regime, and along MONDian ones when $a < a_0$. Baryonic mass determination in the above studies however, are subject to numerous assumptions, as well as uncertainties and systematics, which vary for differing classes of astrophysical systems. Hard to determine gas fractions, star formation histories, the presence of multiple and complex stellar populations and unknown stellar mass functions imply mass to light ratios and their radial variations are subject to large empirical errors.

Here we take a complementary approach, using only kinematical data and avoiding any dynamical physical assumptions or mass estimates in deriving the parameters we study, concentrating merely on the shape of observed projected velocity dispersion profiles. The expected theoretical scalings of both R_M and σ_∞ with M imply the mass can be eliminated to obtain $R_M \propto \sigma_\infty^2$, a relation between the parameters of the directly observable velocity dispersion profiles which can now be directly tested.

By analysing velocity dispersion profiles from Galactic globular clusters recently observed by Scarpa et al. (2007a; 2007b), Scarpa & Falomo (2010) and Scarpa et al. (2011), henceforth the Scarpa et al. group, and Lane et al. (2009), Lane et al. (2010a; 2007b) and Lane et al. (2011), henceforth the Lane et al. group, and elliptical galaxies having high quality 2D kinematics by Falcón-Barroso et al. (2016), using data from the CALIFA project, (Sanchez et al. 2012; Walcher et al. 2014; Sanchez et al. 2016), we show that a universal projected velocity dispersion profile $\sigma(R) = \sigma_0 e^{-(R/R_\sigma)^2} + \sigma_\infty$ adequately serves to model the two distinct classes of astrophysical systems. Further, a scaling of $R_M \propto \sigma_\infty^n$ ensues, with $n = 1.89 \pm 0.32$, compatible with the generic expectations of MONDian gravity models of $n = 2$.

In section (2) we present the development of simple first order predictions for the large scale velocity dispersion expected under MONDian gravity, and the corresponding scalings between the parameters describing such velocity dispersion profiles for pressure supported systems. Section (3) includes a description of the data used for sets of velocity dispersion profiles for globular clusters and elliptical galaxies, together with the fitting procedure and parameters obtained for the universal velocity dispersion profile proposed. In section (4) we show how the two sets of systems treated, spanning seven orders of magnitude in mass, follow the proposed universal velocity dispersion profile, and show also how the flattening radii follow an overall scaling consistent with being proportional to the square of the asymptotic velocity dispersion, as predicted generically under MONDian gravity. Section (5) summarizes our conclusions.

2. MONDIAN THEORETICAL EXPECTATIONS

Thinking of modified gravity in terms of a Newtonian force law implies a change of regime from the Newtonian expression of $F_N = GM/r^2$ to $F_M = (GMa_0)^{1/2}/r$, occurring at scales of $R_M = (GM/a_0)^{1/2}$, if one wants to model observed galactic dynamics in the absence of any dark matter (Milgrom 1983). The details of the transition are not clear, beyond the requirements from consistency with solar system dynamics (Mendoza et al. 2011), Milky Way rotation curve comparisons (Famaey & Binney 2005) and Galactic globular cluster modelling (Hernandez et al. 2012), for the transition to be fairly abrupt. Under such schemes, centrifugal equilibrium velocities will tend to the Tully-Fisher value of:

$$V = (GMa_0)^{1/4}, \quad (1)$$

for test particles orbiting a total baryonic mass M . Under the MONDian regime, the relation between centrifugal equilibrium velocities and isotropic velocity dispersion will be only slightly modified with respect to the Newtonian case, to yield:

$$\sigma_\infty = V/\sqrt{3}, \quad (2)$$

e.g. Milgrom (1984), Hernandez & Jimenez (2012). Thus, we can write the isotropic Maxwellian velocity dispersion of a pressure supported system in the MONDian regime as:

$$\sigma_\infty^2 = \frac{1}{3} (GMa_0)^{1/2}. \quad (3)$$

In order to extend the range over which MONDian dynamics can be tested to the much larger ones over which pressure supported systems appear, would require observations of σ_∞ and independent inferences of the total baryonic mass of various systems, to directly test the validity of equation (3). Any such undertaking will be hindered by the large theoretical uncertainties in total (and radially changing) mass to light ratios, uncertain gas fractions, and details of the relevant IMFs and star formation histories, which to make matters worse, vary significantly from the “simple” cases of globular clusters to the more complex histories of elliptical galaxies. One can circumvent such uncertainties and obtain a simpler empirical test by eliminating M from the above equation in favor of R_M to yield:

$$R_M = \frac{3\sigma_\infty^2}{a_0}, \quad (4)$$

which in astrophysical units reads:

$$\left(\frac{R_M}{pc}\right) = 0.81 \left(\frac{\sigma_\infty}{km/s}\right)^2. \quad (5)$$

The above expression now relates only features of the kinematic velocity dispersion profile of an astronomical

system, as σ_∞ will be the large scale asymptotic projected velocity dispersion profile, and R_M will be the radial scale at which the velocity dispersion profile becomes flat. The above will only make any sense if observed velocity dispersion profiles do indeed show such morphology, for a “Keplerian” decline in an inner Newtonian region, and a transition to a flat velocity dispersion regime on crossing the R_M threshold.

We are inspired to attempt such a comparison across the range of scales covered by pressure supported systems by recent results coming from the observed velocity dispersion profiles of Galactic globular clusters (Scarpa et al. 2010; Scarpa & Falomo 2011) showing precisely such a morphology, and recently shown to comply with Tully-Fisher MONDian expectations (Hernandez et al. 2013a). Further, Desmond (2017) recently demonstrated through an extensive sample of rotation curve observations and baryonic mass inferences across sizes and galactic types, that the inferred mass discrepancy acceleration relation is consistent with MONDian expectations.

In the following section we show a number of velocity dispersion profiles having precisely the morphology described above, for Galactic globular clusters and elliptical galaxies, which we will compare to the expectations of equation (5) in section (4).

Notice also that from equation (4), the resulting combination of parameters $R_M \times \sigma_\infty^2 = GM$ is highly reminiscent of the corresponding Newtonian expression, changing R_M for the half mass radius, and σ_∞ for the central velocity dispersion of a purely Newtonian system (Cappellari et al. 2006; Wolf et al. 2010).

In the above we have assumed that the total baryonic mass has essentially converged, and the dynamical tracers from which σ_∞ is calculated behave as test particles. Although this will never be strictly true, it will hold to a good approximation, given the very centrally concentrated mass profiles of e.g. Galactic globular clusters and the inferred density profiles of close to the de Vaucouleurs surface brightness of elliptical galaxies. Indeed, pressure supported systems have been accurately modeled recently in the MONDian regime reproducing simultaneously the observed surface brightness profiles and the measured velocity dispersion ones, e.g. Galactic globular clusters by Gentile et al. (2010), the giant elliptical galaxy NGC4649 by Jimenez et al. (2013) and tenuous galactic stellar halos by Hernandez et al. (2013b), all in absence of any otherwise dominant dark matter component. More recently, Chae & Gong (2015) studied the predicted distribution of velocity dispersion profiles (VDP) for elliptical galaxies and found that their MONDian models could reproduce the observed distribution of VDP slopes requiring only the observed stellar mass, without any dark matter, and Tian & Ko (2016)

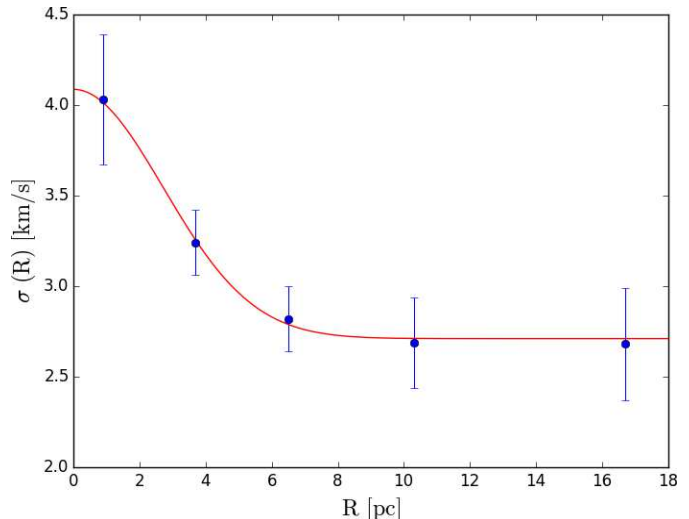


Figure 1. Projected velocity dispersion observations with confidence intervals for globular cluster NGC 6171 as a function of radial distance in the system, with vertical error bars showing the 1σ dispersion at each radial bin. The solid curve gives the best fit to the universal profile proposed. The adequacy of the fit is evident, in spite of the small number of velocity dispersion measurements available.

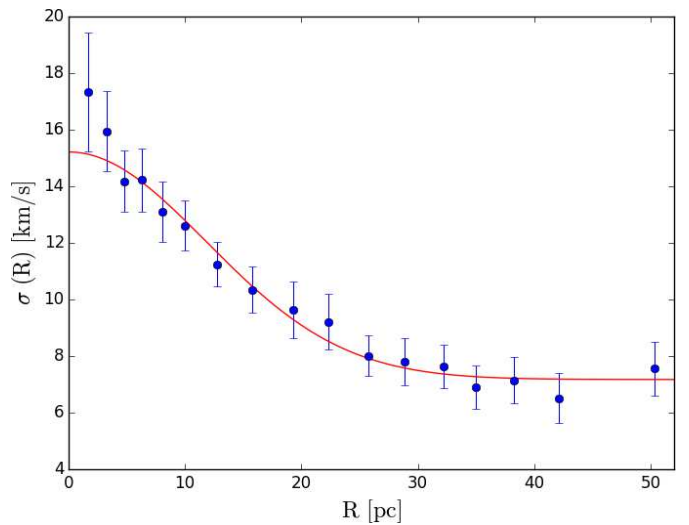


Figure 2. Projected velocity dispersion for globular cluster NGC 5139 as a function of radial distance in the system. The solid curve gives the best fit to the universal profile proposed. The high spatial resolution data reveal no significant deviations from the fit.

concluded that the dynamics of seven elliptical galaxies, as traced by stellar and planetary nebulae, could be well explained by MOND.

3. EMPIRICAL VELOCITY DISPERSION PROFILES

3.1. Galactic globular clusters

In data recently available from the Scarpa et al. group and the Lane et al. group, not only the central values, but the radial projected velocity dispersion profiles for

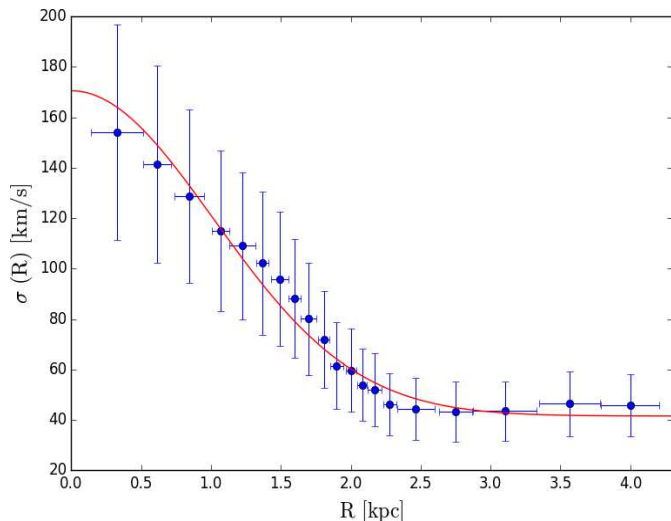


Figure 3. Projected velocity dispersion profile for the elliptical galaxy NGC 0731. The solid curve gives the best fit to the universal profile proposed.

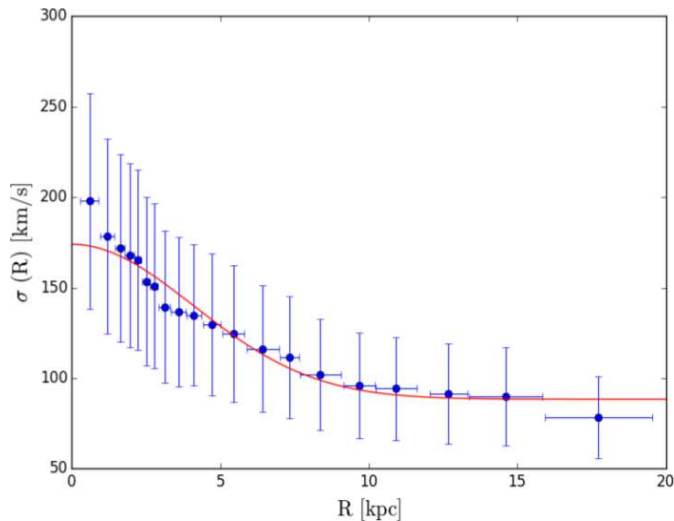


Figure 4. Projected velocity dispersion profile for the elliptical galaxy NGC 6515. The solid curve gives the best fit to the universal profile proposed.

several systems have been published, extending out to several half-light radii. As first mentioned by the Scarpa et al. group, a flattening of the velocity dispersion profiles for Galactic globular clusters appears on crossing the a_0 acceleration threshold, in accordance with MONDian gravity expectations. In Hernandez & Jimenez (2012) some of us recently modeled the above globular cluster data to construct self-gravitating models for the systems studied, where both the projected surface brightness profiles and the observed velocity dispersion profiles have been accurately reproduced, using a modified gravity force law of the type described in section (2). Further, in Hernandez et al. (2013a) we showed that the asymptotic velocity dispersion values for the clusters treated actually match the expected scaling of

$\sigma_\infty \approx (GMa_0)^{1/4}$ of MONDian gravity, through comparing with stellar synthesis models tuned to the ages and metallicities of each of the individual globular clusters studied. In the above works we also showed that an empirical projected velocity dispersion profile of the form:

$$\sigma(R) = \sigma_0 e^{-(R/R_\sigma)^2} + \sigma_\infty \quad (6)$$

serves to accurately model the reported velocity dispersion profiles of Galactic globular clusters. In equation (6) σ_∞ is the asymptotic value for the systems velocity dispersion, the central value for this quantity is given by $\sigma(0) = \sigma_0 + \sigma_\infty$, and R_σ gives a transition radius beyond which the asymptote is rapidly approached.

Here we include again the fits to the data of the Scarpa et al. and Lane et al. groups to equation (6). We use a non-linear least squares Levenberg-Marquardt algorithm to estimate the parameters, and obtain self-consistent 1σ confidence intervals, which are reported in table (1). We have trimmed the total sample used in Hernandez et al. (2013a) to 12 globular clusters where the relative errors in the fitted parameters are in all cases smaller than 50%. This excludes 4 globular clusters with poorly determined velocity dispersion profiles, also keeping the globular cluster sample from growing much beyond the numbers of available well measured systems in the category of low rotation elliptical galaxies. This last to ensure that the systematics relevant to any particular class of objects do not dominate and bias the overall comparisons we attempt.

A first example is shown in figure (1), which shows the observed velocity dispersion profile for the Galactic globular cluster NGC 6171 from the Scarpa et al. group. Also shown is the best fit to equation (6), clearly an excellent empirical representation of the measured profile. A clear “Keplerian decline” in the Newtonian inner region is evident, followed by a transition to a “Tully-Fisher” flat asymptote. Figure (2) gives a second example for NGC 5139, data also from the Scarpa et al. group. Similarly, the adequacy of the fit is evident for this second, significantly larger system. Noticeable is the change in the physical scales of this first two figures. In appendix A we show the velocity dispersion profiles for the remaining systems.

3.2. Elliptical galaxies

A sample of low rotation elliptical galaxies was obtained from Falcón-Barroso et al. (2016), in which 300 radial 2D velocity dispersion profiles were produced from the third data release of the CALIFA survey (Sanchez et al. 2012; Walcher et al. 2014; Sanchez et al. 2016). To ensure that the selected sub-sample was composed of systems with the least dynamical support besides ve-

locity dispersion, we selected galaxies based on their morphology (E0-E3). Our sample comprises only extremely slow rotators, with an average value of a maximum rotation velocity to central sigma per galaxy of $V_{max}/\sigma_0 = 0.213$, very early type systems with negligible total gas content.

We use data directly obtained from Falc3n-Barroso et al. (2016), consisting on 2D radial stellar velocity dispersion observations with their respective uncertainties, as well as associated flux for a correct weighted statistical development. From the 2D velocity dispersion observations we extract a projected radial velocity dispersion representation. Due to the large number of pointings in each galaxy, we averaged the projected velocity dispersion observations within 20 radial bins, obtaining an averaged velocity dispersion profile. As described in Falc3n-Barroso et al. (2016) and Sanchez et al. (2016), velocity dispersion measurements of under 40km/s from the middle resolution setup V1200 are not reliable, so we have discarded these data points in our estimates. Using again a non-linear least squares Levenberg-Marquardt algorithm, we fit the proposed universal function of eq. (6) to the projected velocity dispersion profiles and obtain the equation parameters as well as their respective confidence intervals. After discarding various systems with poorly determined parameters, with fractional errors larger than 50% in the fitted parameters, we compile a final sample of 13 elliptical galaxies, as reported in table (1).

Figures 3 and 4 show the radial binning of the projected 2D radial velocity dispersion of NGC 0731 and NGC 6515 respectively, the former showing the lowest value for the asymptotic flattening of the velocity dispersion profile from our sample, as well as the best fit to the universal function of equation (6). Note again the suitability of the fits in both cases. Appendix A shows the remaining projected velocity dispersion profiles of our sample.

4. COMPARISONS WITH MONDIAN EXPECTATIONS

Comparing figures (1), (2) with figures (3), (4), we see that although the physical scale is changing from pc to kpc, the observed velocity dispersion profiles are clearly self-similar, appearing as scaled versions of each other.

From eq.(6) we see that the central velocity dispersion values, given by $\sigma(0) = \sigma_0 + \sigma_\infty$, span two orders of magnitude, with the scale radii R_σ covering three orders of magnitude, and the total baryonic masses going from a few $10^4 M_\odot$ scale for the smallest Galactic globular clusters to $10^{11} M_\odot$ for the elliptical galaxies. If we now scale the projected velocity dispersion profiles of the various systems presented in the previous section, and consider $\sigma(R)/\sigma_\infty$ as a function of R/R_σ for each

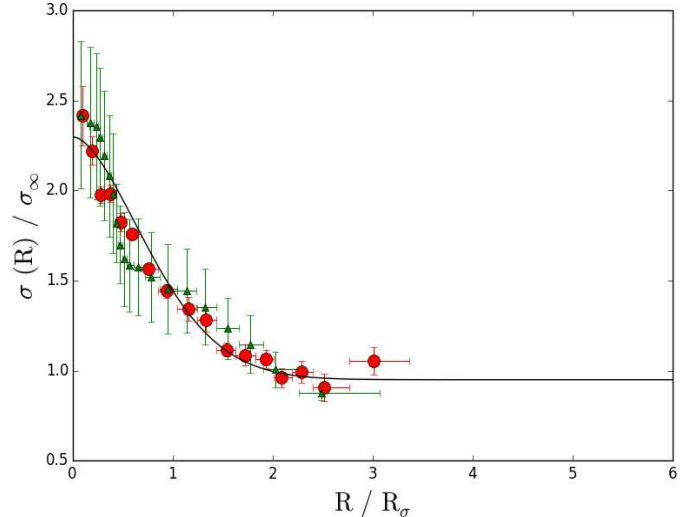


Figure 5. Observed projected velocity dispersion profiles in units of the corresponding σ_∞ values as a function of radius normalized to the corresponding R_σ values, for two distinct systems. Red circles correspond to measurements for the Galactic globular cluster NGC 5139, with a central velocity dispersion of 15.2km/s and $R_\sigma = 16.7\text{pc}$. Green triangles correspond to the elliptical galaxy NGC 0677, with a central velocity dispersion of 195km/s and $R_\sigma = 4.3\text{kpc}$. The consistency of the two scaled projected velocity dispersion profiles is evident, despite the range of scales covered by the comparison.

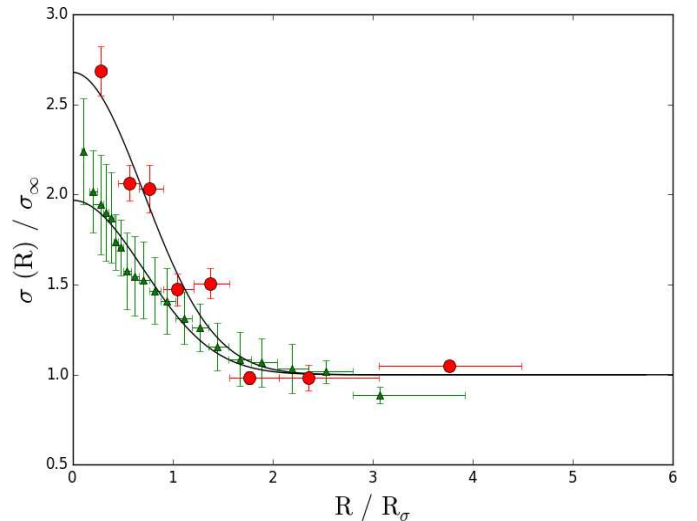


Figure 6. Observed projected velocity dispersion profiles in units of the corresponding σ_∞ values as a function of radius normalized to the corresponding R_σ values, for two distinct systems. Red circles correspond to measurements for the Galactic globular cluster NGC 7078, with a central velocity dispersion of 8.1km/s and $R_\sigma = 8.7\text{pc}$. Green triangles show the elliptical galaxy NGC 6515, with a central velocity dispersion of 174km/s and $R_\sigma = 5.8\text{kpc}$. The two scaled profiles can be modeled through the same functional form of the proposed universal profile, the figure also shows the tendency for the scaled profiles of elliptical galaxies to be flatter and for globular clusters to be steeper.

Table 1. Parameters for velocity dispersion profiles of the the pressure supported systems.

Type of system	Identification	$\sigma_0(km/s)$	$\sigma_\infty(km/s)$	$R_\sigma(pc)$
Globular Cluster	NGC 0104	4.5 ± 0.4	5.0 ± 0.1	14.8 ± 0.9
Globular Cluster	NGC 1851	4.1 ± 1.7	3.9 ± 0.4	7.9 ± 2.3
Globular Cluster	NGC 1904	2.4 ± 0.6	2.0 ± 0.4	10.3 ± 3.3
Globular Cluster	NGC 2419	4.7 ± 0.8	1.0 ± 0.4	1.8 ± 0.3
Globular Cluster	NGC 5139	8.0 ± 0.7	7.2 ± 0.4	16.7 ± 1.9
Globular Cluster	NGC 6171	1.4 ± 0.4	2.7 ± 0.2	3.8 ± 1.1
Globular Cluster	NGC 6218	3.3 ± 0.9	1.4 ± 0.5	4.7 ± 1.2
Globular Cluster	NGC 6341	3.8 ± 0.7	3.1 ± 0.4	6.9 ± 1.4
Globular Cluster	NGC 6656	3.8 ± 1.3	3.3 ± 0.8	7.4 ± 1.7
Globular Cluster	NGC 6752	3.5 ± 0.8	2.0 ± 0.3	10.7 ± 1.4
Globular Cluster	NGC 7078	5.1 ± 1.0	3.0 ± 0.3	8.7 ± 1.7
Globular Cluster	NGC 7099	1.8 ± 0.5	2.2 ± 0.3	6.2 ± 2.3
Elliptical Galaxy	NGC 0155	87.6 ± 25.5	69.1 ± 25.4	$(8.4 \pm 3.6) \times 10^3$
Elliptical Galaxy	NGC 0677	103.6 ± 24.4	91.4 ± 16.7	$(4.3 \pm 1.6) \times 10^3$
Elliptical Galaxy	NGC 0731	129.0 ± 26.9	41.6 ± 6.6	$(1.4 \pm 0.2) \times 10^3$
Elliptical Galaxy	NGC 0938	124.0 ± 25.8	59.0 ± 7.0	$(2.9 \pm 0.5) \times 10^3$
Elliptical Galaxy	NGC 0962	116.3 ± 22.5	57.3 ± 8.5	$(3.7 \pm 0.8) \times 10^3$
Elliptical Galaxy	NGC 1026	123.6 ± 37.7	98.8 ± 8.8	$(1.8 \pm 0.4) \times 10^3$
Elliptical Galaxy	NGC 1060	165.6 ± 18.8	79.5 ± 16.7	$(9.7 \pm 2.0) \times 10^3$
Elliptical Galaxy	NGC 4841A	111.7 ± 46.7	129.9 ± 8.9	$(3.2 \pm 1.4) \times 10^3$
Elliptical Galaxy	NGC 5198	163.6 ± 27.3	53.8 ± 14.7	$(1.5 \pm 0.2) \times 10^3$
Elliptical Galaxy	NGC 5216	105.1 ± 28.3	50.2 ± 9.6	$(1.2 \pm 0.3) \times 10^3$
Elliptical Galaxy	NGC 6515	85.6 ± 24.3	88.4 ± 13.5	$(5.8 \pm 2.2) \times 10^3$
Elliptical Galaxy	NGC 7194	110.4 ± 33.6	132.3 ± 18.7	$(8.0 \pm 3.2) \times 10^3$
Elliptical Galaxy	NGC 7619	151.3 ± 21.8	100.3 ± 14.7	$(4.6 \pm 0.9) \times 10^3$

The first two columns give the object class and identifier for the systems studied. The following three entries show the parameters of the fits to the observed projected velocity dispersion profiles and their confidence intervals. Data from the Scarpa et al. group and the Lane et al. group for Galactic globular clusters, and data from the CALIFA collaboration for elliptical galaxies.

profile, only one degree of freedom remains, given by the central velocity dispersion, $\sigma(0)/\sigma_\infty$.

Therefore, if we choose distinct systems having fixed $\sigma(0)/\sigma_\infty$ values, they should look identical in a $\sigma(R)/\sigma_\infty$ vs. R/R_σ plot. Figure (5) shows the scaled velocity dispersion profiles of two different systems chosen to have very similar $\sigma(0)/\sigma_\infty$ values. Circles correspond to the Galactic globular cluster NGC 5139, while triangles represent data for the elliptical galaxy NGC 0677. The self-similarity of the two quite distinct pressure supported systems is evident, once scaled, and are consistent with each other to within their respective confidence intervals. Actual physical radial scales vary from $R_\sigma = 16.7pc$ of the globular cluster shown to $R_\sigma = 4.3kpc$ of the elliptical galaxy. We see pressure supported systems as showing a simple empirical kinematic profile across many orders of magnitude in scale and distinct classes of systems.

Despite the overlap evident in figure (5), typically we find velocity dispersion profiles for elliptical galaxies to be rather flat, while those of Galactic globular clusters tend to be steeper. This is illustrated in figure (6), which is analogous to figure (5), but shows more typical examples for the two astrophysical systems analysed, the Galactic globular cluster NGC 7078 and the elliptical galaxy NGC 6515. Although the same functional form is evident is evident, the degree of central concentration clearly varies as mentioned above.

We end this section with figure (7), which contains the principal result of our study. The figure shows R_σ and σ_∞ values for the fits to both of the pressure supported systems treated, in a logarithmic plane. The systems shown cover a range of $1.4 - 165.6km/s$ in central velocity dispersion and $1.8pc - 9.7kpc$ in the scale radius R_σ . The two distinct classes of objects are evident, with the small Galactic globular clusters appearing at the low σ_∞

extreme as circles and triangles giving results for elliptical galaxies. The solid line is not a fit to the data but gives the $R_M = 3\sigma_\infty/a_0$ prediction of MONDian gravity of equation (4).

In going from volumetric velocity dispersion profiles to the observable projected velocity dispersion profiles, various projection effects intervene, in ways which depend on the details of the degree of central concentration of the volumetric velocity dispersion profile, and the real space density profiles of the tracers being analyzed (Hernandez & Jimenez 2012; Jimenez et al. 2013a; Tortora 2014). Such details of the integration implicit in obtaining the line of sight projected profiles we treat necessarily introduce changing systematics across both classes of systems, from the centrally peaked kinematics of globular clusters to the flatter ones of elliptical galaxies. To the above we must add the systematics inherent to any comparison across such distinct astrophysical systems over such a range of distances and observational techniques as what we are attempting here. We thus find it encouraging of the physical interpretation presented that the overall trend evident in figure (7) can be clearly well represented by the predictions of equation (4), under the natural identification of $R_\sigma = R_M$, the transition to the flat velocity dispersion regime being given by the length scale of MONDian gravity. Notice that the trend is much less evident within any particular class of objects, only when combining observations across the many orders of magnitude covered in figure (7) does the scaling become clear.

We also performed a weighted linear fit to the data in figure (7). Such a linear fit to the full data set of figure (7), shown in dashed line, yields $R_\sigma = (0.73 \pm 0.13)\sigma_\infty^{1.89 \pm 0.32}$, in clear accordance with the predictions of equation (5) for $A = 0.81$ and $n = 2$. The corresponding fits to only the globular clusters or only the elliptical galaxies yield $A_{GC} = 1.54 \pm 2.35$, $n_{GC} = 1.45 \pm 1.12$ and $A_E = 0.00 \pm 0.81$, $n_E = 3.44 \pm 3.69$, showing that the overall fit is not driven by the position of the two clouds of points, but is actually consistent with the much noisier trends coming from each of the two distinct scale limited classes of objects.

It appears that a unique gravitational physics applies, with a clear transition radius at a R_M scale where the “Keplerian decline” of the inner Newtonian $R < R_M$ region gives way to the “Tully-Fisher” $\sigma(R) \propto (GMa_0)^{1/4}$ of the outer MONDian region, regardless of the fact that we start with self-gravitating systems of stars at pc scales, to the much larger ellipticals at kpc scales.

Increasing our sample size and extending the sample with other type of pressure supported systems, e.g. dSphs, to validate our conclusions is evidently a desirable development, which however must be undertaken with care to keep the number of objects at each class

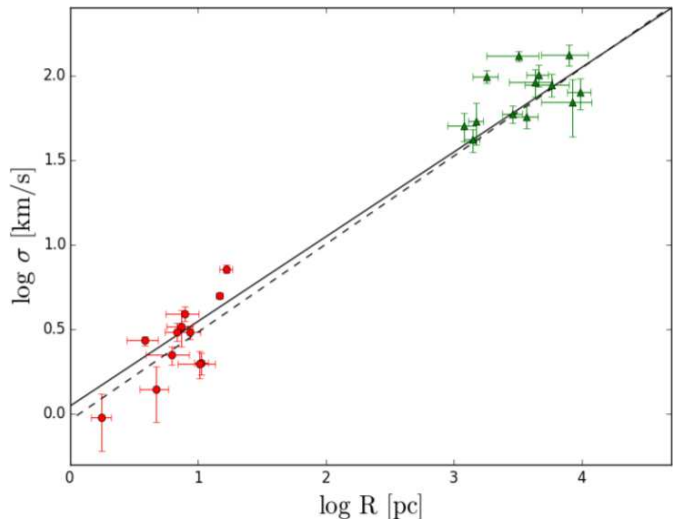


Figure 7. σ_∞ vs. R_σ values for both of the systems treated, red circles for Galactic globular clusters and green triangles for low rotation elliptical galaxies, in a logarithmic plane. The solid line is not a fit to the data, it rather shows the MONDian expectations of equation (4) for the predicted scaling of $R_M = 3\sigma_\infty^2/a_0$, $R_M/pc = 0.81(\sigma_\infty/kms^{-1})^2$. A linear regression fit (dashed line) gives $R_\sigma = (0.73 \pm 0.13)\sigma_\infty^{1.89 \pm 0.32}$, clearly compatible with the theoretical expectation under the identification of $R_\sigma = R_M$.

considered relatively balanced, to make sure that the systematics inherent to any particular class are not biasing conclusions. Similarly, filling the gap present at σ_∞ values of between 10 and 30 km/s would be highly desirable.

5. CONCLUSIONS

A universal projected velocity dispersion profile of $\sigma(R) = \sigma_0 e^{-(R/R_\sigma)^2} + \sigma_\infty$ has been shown to accurately model two distinct classes of astronomical systems; globular clusters and low rotation elliptical galaxies.

MONDian gravity generically predicts $R_M = 3\sigma_\infty^2/a_0$, $R_M/pc = 0.81(\sigma_\infty/kms^{-1})^2$. Data across 7 orders of magnitude in mass give $R_\sigma/pc = A(\sigma_\infty/kms^{-1})^n$, with $A = 0.73 \pm 0.13$ and $n = 1.89 \pm 0.32$.

Thus, in spite of significant observational uncertainties and varying projection effects across apparently very different classes of astronomical systems, the identification of the local physical R_M radius with the empirical projected kinematic R_σ parameter yields results consistent with generic modified gravity expectations, where gravitational anomalies in the $a < a_0$ regime stem from changes in the physics and not a hypothetical dark matter component.

ACKNOWLEDGEMENTS

Xavier Hernandez acknowledges financial assistance from UNAM DGAPA grant IN100814. Reginaldo Durazo acknowledges financial assistance from a CONACyT scholarship. Bernardo Cervantes Sodi ac-

knowledge financial support through PAPIIT project IA103517 from DGAPA-UNAM. SFS thanks the CONACYT-125180, DGAPA-IA100815 and DGAPA-

IA101217 projects for providing him support in this study.

REFERENCES

- Abell, G.O., 1958, *ApJS*, 3, 211
 Barkhouse W. A., Yee H. K. C., Lopez-Cruz O., 2007, *ApJ*, 671, 1471
 Bekenstein J. D., 2004, *Phys. Rev. D*, 70, 083509
 Binney, J., Tremaine, S., 1987, *Galactic Dynamics* (Princeton University Press, Princeton, NJ)
 Bower, R. G., Lucey, J.R., & Ellis, R.S. 1992, *MNRAS*, 254, 601
 Cappellari M., Bacon R., Bureau M., et al., 2006, *MNRAS*, 366, 1126
 Cappellari et al., 2011, *MNRAS*, 413, 813
 Capozziello S., De Laurentis M., 2011, *Phys. Rep.* 509, 167
 Chae K.H., & Gong I.T., 2015, *MNRAS*, 451, 1719
 Desmond H., 2017, *MNRAS*, 464, 4160
 Emsellem et al., 2004, *MNRAS*, 352, 721
 Emsellem et al., 2011, *MNRAS*, 414, 888
 Falcón-Barroso et al., 2016, arXiv:1609.06446
 Gentile G., Famaey B., Angus G., Kroupa, P., 2010, *A&A*, 509, 97
 Hernandez X., Jiménez M. A., 2012, *ApJ*, 750, 9
 Hernandez X., Jiménez M. A., Allen C., 2013a, *MNRAS*, 428, 3196
 Hernandez., Jiménez M. A., Allen C., 2013b, *ApJ*, 770, 83
 Jimenez M. A., Garcia G., Hernandez X., Nasser L., 2013, *ApJ*, 768, 142
 Jones, C., & Forman, W. 1999, *ApJ*, 511, 65
 Famaey B., Binney J., 2005, *MNRAS*, 363, 603
 Famaey B., McGaugh S.S., 2012, *LRR*, 15, 10
 Lane R. R., Kiss L. L., Lewis G. F., Ibata R. A., Siebert A., Bedding T. R., Szekely P., 2009, *MNRAS*, 400, 917
 Lane R. R. et al., 2010a, *MNRAS*, 406, 2732
 Lane R. R., Kiss L. L., Lewis G. F., Ibata R. A., Siebert A., Bedding T. R., Szekely P., 2010b, *MNRAS*, 401, 2521
 Lane R. R. et al., 2011, *A&A*, 530, A31
 Lelli F., McGaugh S. S., Schombert J. M., Pawlowski M. S., 2016, arXiv:161008981
 McGaugh S.S., (2012), *AJ*, 143,40
 McGaugh S.S., Lelli F., Schombert J., (2016), *Phys. Rev. Lett.* 117, 201101
 Mendoza S., Hernandez X., Hidalgo J. C., Bernal T., 2011, *MNRAS*, 411, 226
 Mendoza S., Bernal T., Hernandez X., Hidalgo J. C., Torres L. A., 2013, *MNRAS*, 433, 1802
 Milgrom M., 1983, *ApJ*, 270, 365
 Milgrom M., 1984, *ApJ*, 287, 571
 Rodrigues D. C., de Oliveira P. L., Fabris J. C., Gentile G., 2014, *MNRAS*. 445, 3823
 Sanchez et al., 2012, *A&A*, 538, A8
 Sanchez et al., 2016, *A&A*, 594, A36
 Sanders R. H., McGaugh S. S., 2002, *ARA&A*, 40, 263
 Scarpa R., Marconi G., Gimuzzi R., Carraro G., 2007a, *A&A*, 462, L9
 Scarpa R., Marconi G., Gimuzzi R., Carraro G., 2007b, *The Messenger*, 128, 41
 Scarpa R., & Falomo R., 2010, *A&A*, 523, 43
 Scarpa R., Marconi G., Carraro G., Falomo R., Villanova S., 2011, *A&A*, 525, A148
 Serra A. L., Diaferio A., Murante G., Borgani S., 2011, *MNRAS*, 412, 800
 Swaters R.A., Sanders R.H., McGaugh S S., 2010, *ApJ*, 718, 380
 Tian Y., & Ko C.-M., 2016, *MNRAS*, 462, 1092
 Tortora C., Romanowsky A. J., Cardone V. F., Napolitano N. R., Jetzer Ph., 2014, *MNRAS*, 438, L46
 Walcher et al., 2014, *A&A*, 569, A1
 Wolf J., Martinez G. D., Bullock J. S., et al., 2010, *MNRAS*, 406, 1220
 Verlinde E. P., 2016, arXiv:161102269
 Yahil, A., & Vidal, N. V. 1977, *ApJ*, 214, 347
 York, D. G., et al. 2000, *AJ*, 120, 1579

APPENDIX

A. APPENDIX A: PROJECTED VELOCITY DISPERSION PROFILES

We present projected velocity dispersion profiles for all our sample; 12 globular clusters and 13 elliptical galaxies. Radial scales range from pc for the globular cluster subsample to kpc for elliptical galaxies.

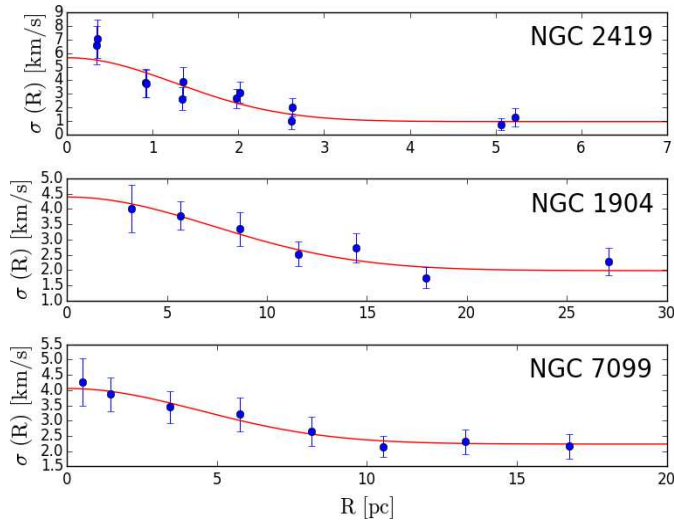


Figure A1. Projected velocity dispersion observations with confidence intervals for three globular clusters as a function of radial distance in the system. The solid curve gives the best fit to the universal profile proposed.

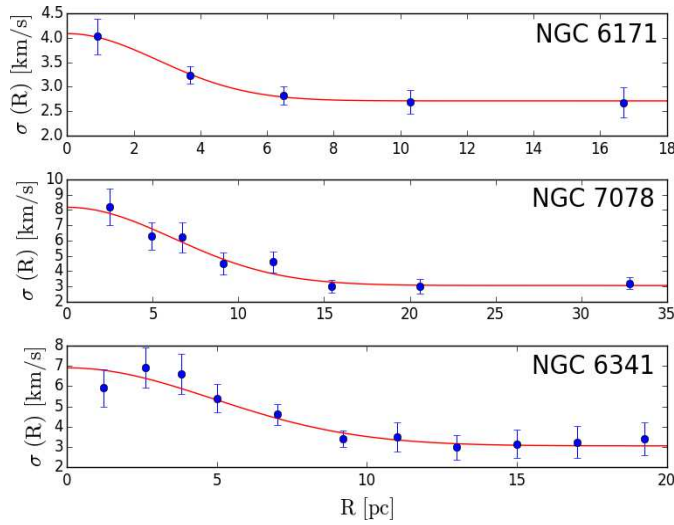


Figure A2. Projected velocity dispersion observations with confidence intervals for three globular clusters as a function of radial distance in the system. The solid curve gives the best fit to the universal profile proposed.

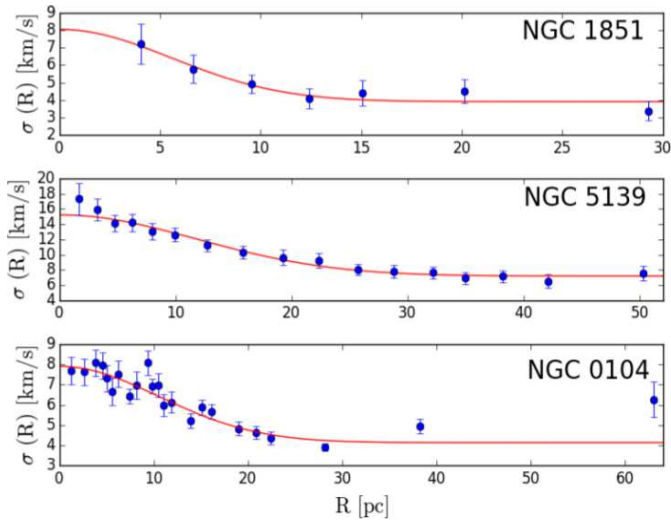


Figure A3. Projected velocity dispersion observations with confidence intervals for two globular clusters as a function of radial distance in the system. The solid curve gives the best fit to the universal profile proposed.

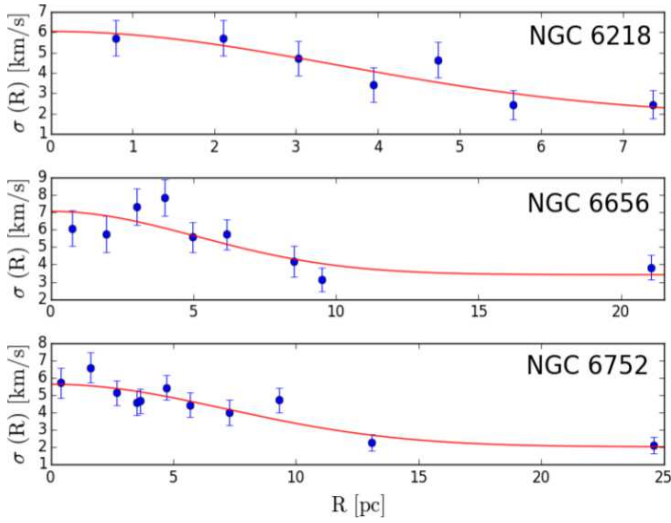


Figure A4. Projected velocity dispersion observations with confidence intervals for two globular clusters as a function of radial distance in the system. The solid curve gives the best fit to the universal profile proposed.

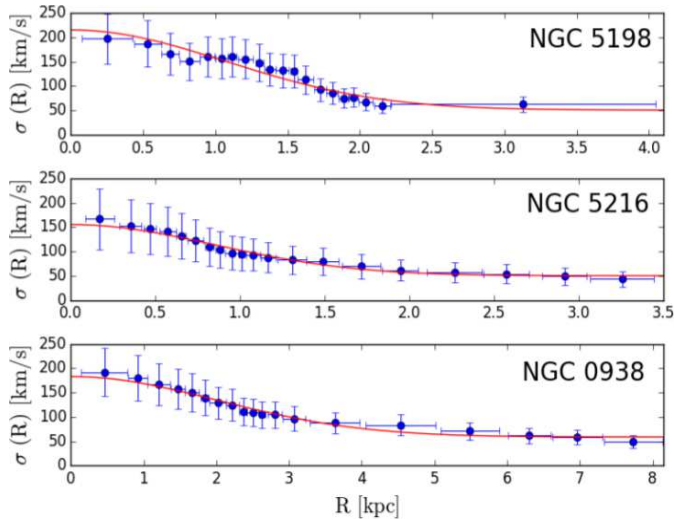


Figure A5. Projected velocity dispersion observations with confidence intervals for three elliptical galaxies as a function of radial distance in the system. The solid curve gives the best fit to the universal profile proposed.

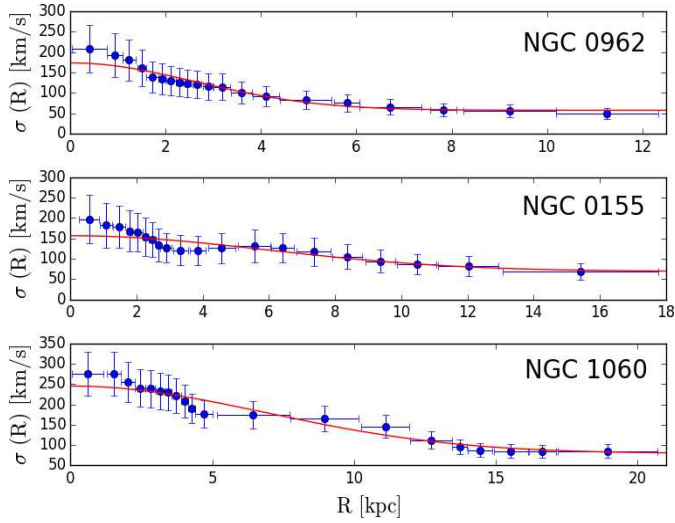


Figure A6. Projected velocity dispersion observations with confidence intervals for three elliptical galaxies as a function of radial distance in the system. The solid curve gives the best fit to the universal profile proposed.

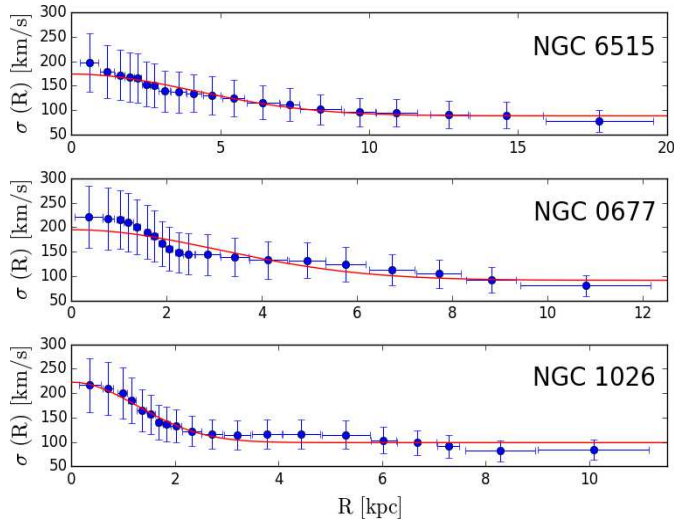


Figure A7. Projected velocity dispersion observations with confidence intervals for three elliptical galaxies as a function of radial distance in the system. The solid curve gives the best fit to the universal profile proposed.

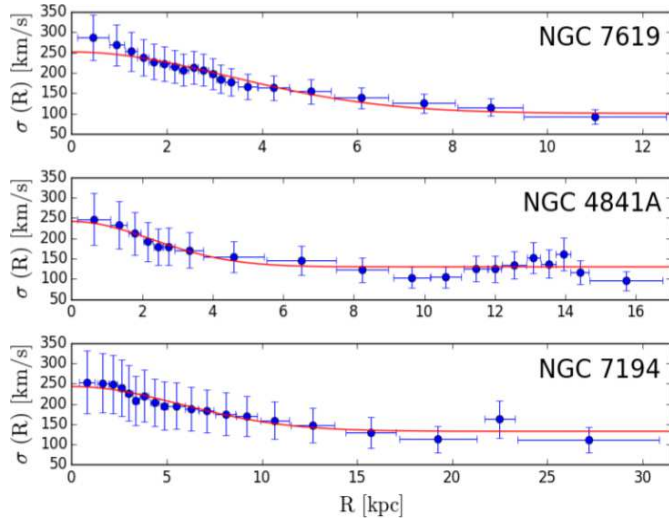


Figure A8. Projected velocity dispersion observations with confidence intervals for three elliptical galaxies as a function of radial distance in the system. The solid curve gives the best fit to the universal profile proposed.